



LAWRENCE  
LIVERMORE  
NATIONAL  
LABORATORY

# Low-Intensity Nonlinear Spectral Effects in Compton Scattering

F. V. Hartemann, F. Albert, C. W. Siders, C. P. Barty

February 24, 2010

Physical Review Letters

## **Disclaimer**

---

This document was prepared as an account of work sponsored by an agency of the United States government. Neither the United States government nor Lawrence Livermore National Security, LLC, nor any of their employees makes any warranty, expressed or implied, or assumes any legal liability or responsibility for the accuracy, completeness, or usefulness of any information, apparatus, product, or process disclosed, or represents that its use would not infringe privately owned rights. Reference herein to any specific commercial product, process, or service by trade name, trademark, manufacturer, or otherwise does not necessarily constitute or imply its endorsement, recommendation, or favoring by the United States government or Lawrence Livermore National Security, LLC. The views and opinions of authors expressed herein do not necessarily state or reflect those of the United States government or Lawrence Livermore National Security, LLC, and shall not be used for advertising or product endorsement purposes.

# Low-Intensity Nonlinear Spectral Effects in Compton Scattering

Fred V. Hartemann, Félicie Albert, Craig W. Siders and Christopher P.J. Barty  
Lawrence Livermore National Laboratory, Livermore, CA, 94550

(Dated:)

Nonlinear effects are known to occur in Compton scattering light sources, when the laser normalized 4-potential,  $A = e\sqrt{-A_\mu A^\mu}/m_0c$  approaches unity. In this letter, it is shown that nonlinear spectral features can appear at arbitrarily low values of  $A$ , if the fractional bandwidth of the laser pulse,  $\Delta\phi^{-1}$ , is sufficiently small to satisfy  $A^2\Delta\phi \approx 1$ . A three dimensional analysis, based on a local plane-wave, slow-varying envelope approximation, enables the study of these effects for realistic interactions between an electron beam and a laser pulse, and their influence on high-precision Compton scattering light sources.

PACS numbers: 07.85.-m, 41.60.Cr, 41.60-m, 42.72.-g

Rapid advances in terawatt-class laser technology [1] and high-brightness, high-gradient electron accelerators [2] are enabling the development of a new type of light source based on Compton scattering [3], where relativistic electrons interact with a coherent photon field to generate bright, ultrafast, tunable x-rays and  $\gamma$ -rays [4, 5]. These compact sources are a natural complement to larger-scale 3<sup>rd</sup> and 4<sup>th</sup> generation light sources [6], and provide a mean to generate MeV-scale photons with unprecedented spectral brightness.

Among other important features, such as wide tunability and ultrashort pulse capability, Compton scattering x-ray and  $\gamma$ -ray sources offer the potential of generating highly correlated, narrow-band radiation in a very small solid angle. This characteristic is desirable for a number applications, including nuclear resonance fluorescence (NRF) [7] or protein crystallography [8]. Therefore, the focus of this work is the physical origin of spectral broadening mechanisms in Compton scattering, with a special emphasis on nonlinear effects and recoil, and their influence on the performance of high-precision Compton scattering light sources.

In this letter, four novel results are presented. 1) A new derivation of the nonlinear electron dynamics in a plane-wave is described. 2) A covariant form of the radiation formula is given, including a quantum correction term shown to yield the proper recoil for the interaction, along with a gauge invariant, covariant definition of the 4-polarization [9]. 3) We demonstrate that, while nonlinear effects are known to occur in light sources when the wiggler parameter, of normalized 4-potential  $A = e\sqrt{-A_\mu A^\mu}/m_0c$ , approaches unity, nonlinear spectral features can also appear at arbitrarily low values of  $A$ , if the fractional bandwidth of the laser pulse,  $\Delta\phi^{-1}$ , is sufficiently small and satisfies the condition  $A^2\Delta\phi \approx 1$ . 4) A fully three-dimensional (3D) analysis of nonlinear effects in the long-pulse regime is given, based on a local plane-wave, slow-varying envelope approximation.

The Lorentz force equation is:  $du_\mu/d\tau = -(\partial_\mu A_\nu - \partial_\nu A_\mu)u^\nu$ ;  $u_\mu = dx_\mu/d\tau$  is the electron 4-velocity, and  $A_\mu$  is the radiation 4-potential. If  $\sqrt{-A_\mu A^\mu} = A \ll 1$ , this equation can be solved by perturbation: let  $u_\mu = u_\mu^0 + u_\mu^1 + \dots$ , where  $u_\mu^n \propto A^n$ ;

$$\frac{du_\mu^1}{d\tau} = -(\partial_\mu A_\nu - \partial_\nu A_\mu)u_0^\nu, \quad \frac{du_\mu^{n+1}}{d\tau} = -(\partial_\mu A_\nu - \partial_\nu A_\mu)u_n^\nu. \quad (1)$$

Here,  $u_\mu^0$  corresponds to ballistic electron trajectories, re-

flecting covariance. This system can be solved in momentum space, where dynamical quantities are Fourier transformed as:  $4\pi^2 f(x^\nu) = \int \tilde{f}(k_\nu) e^{ik_\nu x^\nu} d^4k$ . Diagonalizing the system, the 1<sup>st</sup> order yields [8]:  $\tilde{u}_\mu^1 ik_\nu dx^\nu/d\tau = -u_0^\nu i(k_\mu \tilde{A}_\nu - k_\nu \tilde{A}_\mu)$ . Approximating  $dx^\nu/d\tau = u^\nu$  by  $u_0^\nu$  to balance the perturbation order, one obtains:  $\tilde{u}_\mu^1 = \tilde{A}_\mu - k_\mu \frac{A_\nu u_0^\nu}{k_\nu u_0^\nu}$ .

In the case of a plane wave, let us show that the 2<sup>nd</sup> order solution corresponds to the exact nonlinear solution [10], while all other perturbation orders are null. In Fourier space,  $u_\mu^2 i2k_\nu dx^\nu/d\tau = -i(k_\mu A_\nu - k_\nu A_\mu)[A^\nu - k^\nu (A_\lambda u_0^\lambda)/(k_\lambda u_0^\lambda)]$ . The factor 2 on the left hand side corresponds to the 2<sup>nd</sup> harmonic. To keep the order in  $A^n$  balanced,  $dx^\nu/d\tau \approx u_0^\nu$ ; contracting terms, one obtains:

$$u_\mu^2 i2k_\nu u_0^\nu = -k_\mu \left[ A_\nu \left( A^\nu + k^\nu \frac{A_\lambda u_0^\lambda}{k_\lambda u_0^\lambda} \right) \right] + A_\mu \left[ k_\nu \left( A^\nu - k^\nu \frac{A_\lambda u_0^\lambda}{k_\lambda u_0^\lambda} \right) \right]. \quad (2)$$

Using  $k_\nu A^\nu = 0$  (Lorentz gauge), and  $k_\nu k^\nu = 0$  (dispersion relation),  $u_\mu^2 = -k_\mu \frac{A_\nu A^\nu}{2k_\nu u_0^\nu}$ . Using the same approach for higher order terms, we have  $u_\mu^n i n k_\nu u_0^\nu = -i(k_\mu A_\nu - k_\nu A_\mu)u_{n-1}^\nu$ ; in particular,

$$u_\mu^3 3ik_\nu u_0^\nu = -i(k_\nu A_\nu - k_\nu A_\mu u_2^\nu) = i(k_\nu A_\nu - k_\nu A_\mu u_2^\nu) k_\mu \frac{A_\nu A^\nu}{2k_\nu u_0^\nu} = 0, \quad (3)$$

for the 3<sup>rd</sup> order. All perturbation orders are null beyond  $n = 2$ , and we recover the exact nonlinear plane wave solution [10]:  $u_\mu = u_\mu^0 + A_\mu - k_\mu [A_\nu (A^\nu + 2u_0^\nu)/2k_\nu u_0^\nu]$ .

Nonlinear spectra can be derived from this result: the covariant radiation formula describes the number of photons scattered per unit frequency and solid angle:

$$\frac{d^2N}{dq d\Omega} = \frac{\alpha}{4\pi^2} q \left| \int_{-\infty}^{+\infty} \pi_\mu u^\mu e^{-iq_\nu x^\nu} d\tau \right|^2. \quad (4)$$

$\alpha$  is the fine structure constant;  $\pi_\mu$  and  $q_\mu$  are the 4-polarization and the 4-wavenumber of the scattered radiation;  $x_\mu(\tau)$  is the electron 4-trajectory. For an incident plane wave, it is useful to use the electron phase,  $\phi = k_\mu x^\mu$ , as the independent variable. Contracting  $u_\mu$  by  $k_\mu$ , the incident light cone

variable [11],  $\kappa = d\phi/d\tau$ , is shown to be constant:  $\kappa = k_\mu u_\mu^0$ . Eq. 4 now reads:

$$\frac{d^2N}{dq d\Omega} = \frac{\alpha}{4\pi^2} \frac{q}{\kappa^2} \left| \pi_\mu \int_{-\infty}^{+\infty} u^\mu(\phi) e^{-iq_\nu \int \frac{u^\nu}{\kappa} d\psi} d\phi \right|^2. \quad (5)$$

To account for recoil, consider a monochromatic incident plane wave with vanishingly small amplitude  $a_\mu A_0 e^{i\phi}$ ; adding the quantum correction  $\lambda k_\mu$  yields  $u_\mu = \kappa dx_\mu/d\phi = u_\mu^0 + A_\mu - k_\mu \frac{A_\nu u_\nu^0}{k_\nu u_\nu^0} + \lambda k_\mu$ , which integrates to  $x_\mu - x_\mu^0 = \kappa^{-1}(u_\mu^0 + \lambda k_\mu)\phi$ . Here,  $\lambda = \hbar/m_0c$  is the reduced Compton wavelength of the electron. Defining the incident 4-polarization in a covariant, gauge invariant manner [9], as  $\epsilon_\mu = \frac{1}{\sqrt{-A_\nu A^\nu}}(A_\mu - k_\mu \frac{A_\nu u_\nu^0}{k_\nu u_\nu^0})$ , the scattered radiation spectral density is:

$$\frac{d^2N}{dq d\Omega} = \frac{\alpha}{4\pi^2} \frac{q}{\kappa^2} A_0^2 |e^{-iq_\nu x_\nu^0}|^2 \left| \pi_\mu \epsilon^\mu \right|^2 \left| \int_{-\infty}^{+\infty} e^{i\phi(1 - \frac{\lambda + \lambda q_\nu k^\nu}{\kappa})} d\phi \right|^2. \quad (6)$$

Eq. 6 contains the coherence factor [12], the dipole radiation pattern, and a Dirac delta function spectrum centered at a frequency satisfying the condition:  $\kappa - \lambda = \lambda q_\mu k^\mu$ , where  $\lambda = q_\mu u_\mu^0$  is the scattered light cone variable [11]. Importantly, this condition satisfies the Compton formula [3]: considering energy-momentum conservation, we have:  $u_\mu^0 + \lambda k_\mu = v_\mu + \lambda q_\mu$ , where  $v_\mu$  is the electron 4-velocity after the interaction. Since  $v_\mu v^\mu = 1$ ,  $[u_\mu^0 + \lambda(k_\mu - q_\mu)][u_\mu^0 + \lambda(k^\mu - q^\mu)] = 1$ , the sought after result is obtained using  $u_\mu^0 u_\mu^0 = 1$ ,  $k_\mu k^\mu = 0$  and  $q_\mu q^\mu = 0$ . Moreover, in the classical limit where  $\lambda \rightarrow 0$ , the Thomson scattering formula is recovered. Eq. 5 can now be used to study nonlinear spectra. First, let  $A_\mu = A_0(a_\mu \sin \phi + \sigma b_\mu \cos \phi)$  with  $a_\mu a^\mu = b_\mu b^\mu = -1$  and  $a_\mu b^\mu = a_\mu k^\mu = b_\mu k^\mu = 0$ ;  $\sigma = 0, \pm 1$  correspond to linear or circular polarization states. Contracting the 4-trajectory with the scattered 4-wavenumber leads to the nonlinear phase in the radiation formula:

$$\begin{aligned} q^\mu x_\mu &= q^\mu x_\mu^0 + \frac{1}{\kappa} \phi \left[ \lambda + k_\mu q^\mu \left( \lambda n + \frac{\langle -A_\nu A^\nu \rangle}{2\kappa} \right) \right] \\ &+ \frac{1}{\kappa} \cos \phi A_0 \left( \frac{u_\nu^0 a^\nu}{\kappa} k_\mu - a_\mu \right) q^\mu \\ &+ \frac{1}{\kappa} \sin \phi A_0 \sigma \left( \frac{u_\nu^0 b^\nu}{\kappa} k_\mu - b_\mu \right) q^\mu \\ &+ \sin 2\phi \frac{k_\mu q^\mu}{2\kappa^2} \frac{\sigma^2 - 1}{4}. \end{aligned} \quad (7)$$

The average is over a cycle; the non-zero average of the  $2^{nd}$  harmonic motion corresponds to the dressed electron mass. Eq. 7 can be understood by examining its periodicity: the first and second terms are periodic in  $\phi$ ; the linear term in  $\phi$  becomes periodic if the resonance condition  $\kappa^{-1} q_n^\mu (u_\mu^0 + \lambda n k_\mu + \frac{1}{2} \kappa^{-1} k_\mu \langle -A_\nu A^\nu \rangle) = n \in \mathbb{N}$  is satisfied. This defines a series of harmonics:  $n\kappa - \lambda = k_\mu q_n^\mu (n\lambda + \frac{1}{2} \kappa^{-1} k_\mu \langle -A_\nu A^\nu \rangle)$ . For head-on collisions,  $k_\mu = (k, 0, 0, k)$ ,  $u_\mu = (\cosh \rho, 0, 0, -\sinh \rho)$ ; and on axis radiation,  $q_n^\mu = (q_n, 0, 0, q_n)$ , one finds:  $q_n = n\kappa e^{2\rho}/(1 +$

$\langle -A_\nu A^\nu \rangle + 2e^\rho n\lambda k)$ , where  $e^{2\rho}$  is the Doppler upshift;  $\langle -A_\nu A^\nu \rangle$  is the radiation pressure; and  $2e^\rho n\lambda k$  is the recoil term.

It is well worth comparing this result with the nonlinear multi-photon Compton formula. 4-momentum conservation yields:  $u_\mu + \lambda(k_\mu^1 + k_\mu^2 + \dots k_\mu^n) = v_\mu + \lambda q_n^\mu$ . For coherent plane waves,  $k_\mu^1 = \dots k_\mu^n$ , which leads to considerable simplification:  $v_\mu = u_\mu + \lambda(nk_\mu - q_n^\mu)$ . Taking the square of this expression, and assuming the fact that  $u_\mu u^\mu = v_\mu v^\mu = 1$  and  $k_\mu k^\mu = q_n^\mu q_n^\mu = 0$ , we first have  $u^\mu(nk_\mu - q_n^\mu)$ . Now replacing  $u_\mu$  by the nonlinear solution derived earlier:

$$\begin{aligned} \left( u_\mu^0 + A_\mu - k_\mu \frac{A_\nu A^\nu + 2u_\nu^0 A^\nu}{2u_\nu^0 k^\nu} \right) (nk^\mu - q_n^\mu) &= \lambda n k_\mu q_n^\mu; \quad (8) \\ nu_\mu^0 k^\mu - \left( u_\mu^0 - \frac{k_\mu}{2u_\nu^0 k^\nu \langle A_\nu A^\nu \rangle} \right) q_n^\mu &= \lambda n k_\mu q_n^\mu. \end{aligned}$$

Comparing this result to the previous resonance condition clearly establishes the connection between harmonics and multi-photon interactions.

In the case of a plane wave with an envelope,  $g(\phi)$ , it can be shown that for on-axis radiation, the linear transverse oscillations do not contribute to the radiation phase if the wave is counter-propagating with respect to the electron. The total phase is:

$$\begin{aligned} \Phi &= q_\mu(x^\mu - x_\mu^0) = \frac{\phi}{\kappa} (q_\mu u_\mu^0 + \lambda q_\mu k^\mu) \\ &+ \frac{q_\mu k^\mu}{2\kappa^2} A_0^2 \int g^2(\phi) (\sin^2 \phi + \sigma^2 \cos^2 \phi) d\phi. \end{aligned} \quad (9)$$

Furthermore, an exact analytical result can be obtained for a circularly polarized hyperbolic secant pulse, where  $g(\phi) = \text{sech}\left(\frac{\phi}{\Delta\phi}\right)$ :

$$\begin{aligned} \Phi - \frac{q_\mu}{\kappa} (u_\mu^0 + \lambda k^\mu) \phi &= \frac{q_\mu k^\mu}{2\kappa^2} A_0^2 \int_{-\infty}^{\phi} \text{sech}^2\left(\frac{\psi}{\Delta\phi}\right) d\psi \\ &= \frac{q_\mu k^\mu}{2\kappa^2} A_0^2 \Delta\phi \left[ 1 + \tanh\left(\frac{\phi}{\Delta\phi}\right) \right] \end{aligned} \quad (10)$$

This clearly shows the  $A_0^2 \Delta\phi$  scaling of the nonlinear phase. Choosing the interaction region so that  $k_\mu = (k, 0, 0, k)$ ,  $u_\mu = (\cosh \rho, 0, 0, -\sinh \rho)$  and  $q_\mu = (q, 0, 0, -q)$ , the radiation integral reads:

$$\begin{aligned} \frac{d^2N}{dq d\Omega} &= \frac{\alpha}{4\pi^2} \frac{\chi}{k} \\ &\times \left| A_0 e^{i\chi A_0^2 \Delta\phi} \int_{-\infty}^{\infty} \frac{\mathbf{x} \sin \phi + \mathbf{y} \cos \phi}{\cosh(\phi/\Delta\phi)} \exp \left\{ i\chi \left[ \phi(1+r) + A_0^2 \Delta\phi \tanh \frac{\phi}{\Delta\phi} \right] \right\} d\phi \right|^2 \end{aligned} \quad (11)$$

Here,  $\chi = qe^{2\rho}/k$  is the normalized Doppler-shifter (Thomson scattering) frequency, and  $r = 2\lambda ke^\rho$  is the recoil. we note that for linear polarization,  $A_0^2$  can be replaced by  $\langle A_0^2 \rangle = \frac{1}{2} A_0^2$ . Two changes of variable lead to an analytically tractable

integral [13]; first, let  $x = e^{\phi/\Delta\phi}$ ; next, set  $z = (x^2 - 1)/(x^2 + 1)$ , to obtain:

$$\begin{aligned} \frac{d^2 N}{dq d\Omega} &= \frac{\alpha}{4\pi^2} \frac{\chi}{k} \\ &\left| \int_{-1}^{+1} (1+z)^{-\frac{1}{2}-\frac{1}{2}\Delta\phi[\chi(1+r)\pm 1]} (1-z)^{-\frac{1}{2}+\frac{1}{2}\Delta\phi[\chi(1+r)\pm 1]} (\mathbf{y} \pm i\mathbf{x}) e^{iA_0^2\Delta\phi\chi z} dz \right|^2 \\ &= \frac{\alpha}{2} \frac{\chi}{k} A_0^2 \\ &\times \sum \left| L_{\frac{1}{2}\Delta\phi[\chi(1+r)\pm 1]-\frac{1}{2}}(2iA_0^2\Delta\phi\chi) \right|^2 \operatorname{sech}^2 \left\{ \frac{\pi\Delta\phi}{2} [\chi(1+r) \pm 1] \right\} \end{aligned} \quad (13)$$

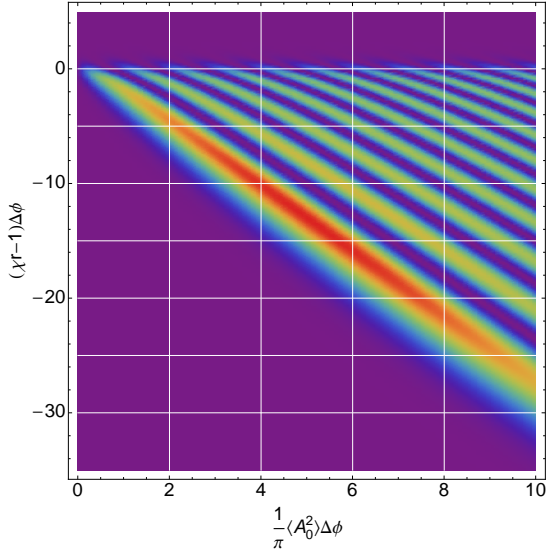


FIG. 1. Scale invariant nonlinear spectrum

Here,  $L_n(x)$  is the  $n^{\text{th}}$  Laguerre polynomial [14]. The behavior of this solution is shown in Fig. 1, where the scale-invariant nonlinear spectrum is plotted as a function of  $\langle A_0^2 \rangle \Delta\phi/\pi$ , and  $\Delta\phi[\chi(1+r) \pm 1]$ . The downshifting due to radiation pressure is evident, and the number of spectral lines is equal to the nonlinear phase accumulated over the pulse,  $A_0^2\Delta\phi[\lim_{\phi \rightarrow +\infty} \tanh(\phi/\Delta\phi) - [\lim_{\phi \rightarrow -\infty} \tanh(\phi/\Delta\phi)]] = 2A_0^2\Delta\phi$ , divided by  $2\pi$ . In addition, the amplitude of the main spectral line first scales quadratically with  $A_0$ , then reaches a maximum, and slowly decays, as the scattered energy is distributed over an increasing number of spectral lines. The underlying physics can be understood as follows: the inhomogeneous radiation pressure leads to a slow dephasing between the electron and the scattered radiation that accumulates over the entire interaction; if the nonlinear phase integral is large enough, interference effects result in discrete anharmonic lines. Alternatively, one can think of this process as a competition between the bandwidth of the laser and nonlinear dephasing: if the laser spectrum is narrow enough, one can resolve increasingly small nonlinear effects.

We now focus on the interplay between 3D effects, the electron phase space, and the nonlinear inhomogeneous ra-

diation pressure. To accurately simulate realistic interactions between a high brightness electron beam and a laser pulse, and study their influence on high-precision Compton scattering light sources, a fully 3D code is required. For long, narrow-band laser pulses, a direct approach, accounting for fine details in the correlated electron beam phase space [15], is computationally intensive. Instead, one can take advantage of the slow-varying pulse envelope, paraxial, and weakly nonlinear approximations to develop a local plane-wave model leading to analytical expressions for the electron 4-trajectory. The corresponding three small parameters are:  $\Delta\phi^{-1}$ ,  $\epsilon = (k_0 w_0)^{-1}$ , and  $A_0$ , respectively. For large Doppler upshifts, these conditions ensure that the particle excursions from ballistic trajectories are very small compared to all other scales characterizing the system. In turn, this allows the use of a local plane wave model, where all dynamical variables become functions of  $\phi$ : the 6-dimensional input phase space specifies a ballistic trajectory for a given electron,  $x_\mu^i(\phi) = x_\mu^{0i} + \phi(u_\mu^{0i}/k_i)$ ; all other dynamical quantities are evaluated along this 4-trajectory.

A Fourier transform-limited Gaussian laser pulse and a 6-dimensional uncorrelated Gaussian electron beam phase space are modeled here to provide a baseline example; the general method will be the object of another paper. The three-dimensional electromagnetic fields are generated from the vector  $\mathbf{G}$ , by taking  $\mathbf{A} = \nabla \times \mathbf{G}$ , thus ensuring a divergence-free potential vector satisfying the Coulomb gauge. The electric field is given by  $\mathbf{E} = -\partial_t \mathbf{A}$ , while the magnetic induction is  $\mathbf{B} = \nabla \times \mathbf{A}$ . In the case of a Gaussian pulse propagating paraxially along the positive  $z$ -axis, focused cylindrically, and polarized along the  $x$ -axis, the generating function is [16]:

$$G_y = A_0 e^{-\frac{\phi^2}{\Delta\phi^2} - \frac{r^2}{1+z^2}} \cos \left[ -\phi - z \frac{r^2}{1+z^2} - \operatorname{atan}(z) \right] / k_0 \sqrt{1+z^2}. \quad (14)$$

Here,  $A_0$  is the amplitude of the vector potential;  $k_0 = \omega_0/c$  is the central wavenumber of the pulse. Space-time coordinates are normalized as follows:  $r \rightarrow r/w_0$ ,  $z \rightarrow z/z_0$ ,  $t \rightarrow ct/z_0$ ,  $z_0 = \frac{1}{2}k_0 w_0^2$  is the Rayleigh range,  $w_0$  is the focal waist,  $\phi = \omega_0 t - k_0 z$  is the phase, and  $\Delta\phi = \omega_0 t$ . Using both the slow-varying envelope and the paraxial approximations, and systematically neglecting higher order terms, the 4-potential is derived. Replacing all space-time coordinates by their values along ballistic trajectories, the local 4-velocity can be evaluated by keeping terms of order  $A_0$ ,  $A_0\epsilon$ , and  $A_0^2$ ; for example, the component parallel to the polarization is:

$$\begin{aligned} u_x(\phi) &= u_{x0} + A_0 \frac{\exp \left[ -\frac{\phi^2}{\Delta\phi^2} - \frac{r(\phi)^2}{1+z(\phi)^2} \right]}{\sqrt{1+z(\phi)^2}} \\ &\times \left[ 1 + 4\epsilon \frac{u_{x0}}{\gamma_0 - u_{z0}} \frac{x(\phi)z(\phi)}{1+z(\phi)^2} \right] \sin[-\phi - \psi(\phi)], \end{aligned} \quad (15)$$

where  $\psi = -z[r^2/(1+z^2)] + \operatorname{atan}(z)$ .

Fig. 2 shows typical trajectories and radiation pressure integrals obtained using this approach. Beyond this point, the flow of the 3D code can be summarized as follows. All dynamical

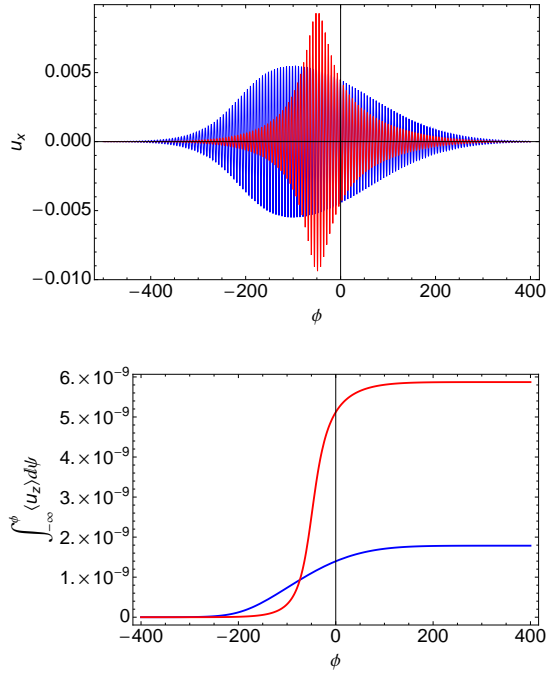


FIG. 2. Top: transverse electron momentum as a function of phase. Simulation parameters:  $\gamma_0 = 100$ ,  $A_0 = 0.01$ ,  $\Delta\phi = 200$ ,  $x_i = y_i = 0$ ,  $z_i = -2$ ,  $u_{x0} = u_{y0} = 0.01$ ,  $\epsilon = 0.01$  (blue),  $\epsilon = 0.025$  (red). Bottom: corresponding non linear radiation pressure integrals.

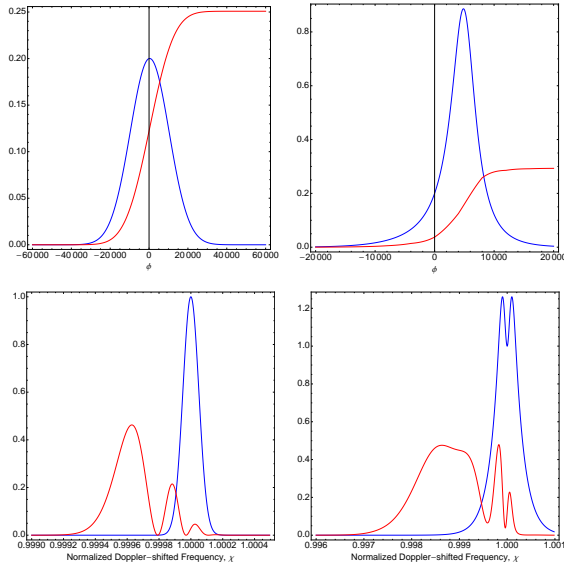


FIG. 3. Top: (blue) laser pulse seen by the electron and (red) non-linear radiation pressure. Bottom: corresponding linear (blue) and nonlinear (red) spectra. Parameters are the same unless noted. Left:  $\gamma_0 = 500$ ,  $A_0 = 0.05$ ,  $\Delta\phi = 20000$ ,  $x_i = y_i = u_{x0} = u_{y0} = 0$ ,  $z_i = 2$ ,  $\epsilon = 1/500$ ; right:  $\epsilon = 1/50$ .

quantities are separated into slow-varying components and periodic functions; integrals over the phase are performed using the approximation:  $\int f p d\phi \approx \langle p \rangle \int f d\phi + f \int (p - \langle p \rangle) d\phi$ , where  $p(\phi + 2\pi) = p(\phi)$ , and where the average is defined as  $\langle p \rangle = \frac{1}{2\pi} \int_{-\pi}^{\pi} p d\phi$ . For harmonic functions,  $\int (p - \langle p \rangle) d\phi$  is analytical, while the integral over  $f$  can be performed efficiently because it is a slow-varying function. This approximation is used to evaluate the 4-trajectory and the radiation integral. For situations dominated by diffraction (Fig. 3 left), the Fourier transform of the asymmetric Lorentzian envelope yields complex nonlinear spectra. Finally, for a 6N-dimensional distribution of input particles in phase space, the radiation is obtained by incoherent summation; linear (blue) and nonlinear (red) spectra are shown in Fig. 4. Full 3D trajectories are used for all cases, the linear spectra are calculated from the ballistic phase  $\frac{q\mu}{\kappa} (u_0^\mu + \lambda k^\mu) \phi$  only. Even for  $A_0^2 = 2.5 \times 10^3 \ll 1$ , the difference between linear and nonlinear spectra is clearly established, both for an idealized electron beam and for a realistic case.

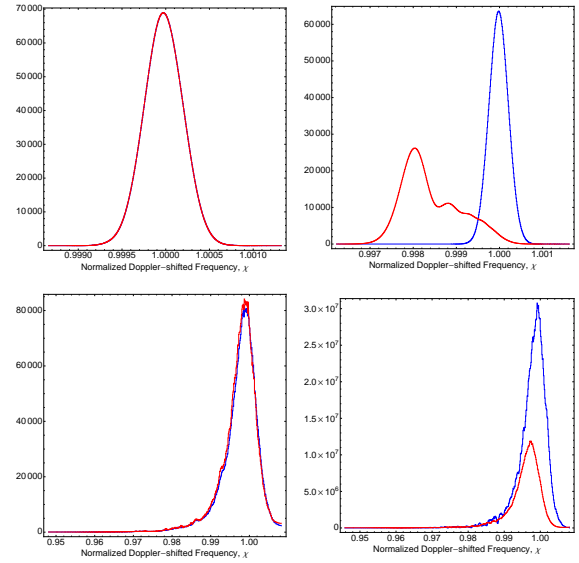


FIG. 4. From top left, clockwise. All parameters are the same unless specified: Benchmark case:  $A_0^2 = 10^{-6}$ ,  $\Delta\phi = 10000$ ,  $\epsilon = 1/2000$ ,  $\lambda_0 = 532$  nm,  $\Delta\tau = 2.5$  ps,  $\gamma_0 = 500$ ,  $\Delta\gamma/\gamma_0 = 0.01\%$ ,  $\epsilon_n = 10^{-7}$ ,  $r_b = 20$   $\mu$ m. idealized case:  $A_0^2 = 2.5 \times 10^{-3}$ . Realistic case:  $A_0^2 = 2.5 \times 10^{-3}$ ,  $\epsilon = 1/250$ ,  $\Delta\gamma/\gamma_0 = 0.1\%$ ,  $\epsilon_n = 10^{-6}$ . Diffraction dominated case:  $A_0^2 = 2.5 \times 10^{-3}$ ,  $\epsilon = 1/20$ ,  $\Delta\gamma/\gamma_0 = 0.1\%$ ,  $\epsilon_n = 10^{-6}$ .

This work performed under the auspices of the U.S. Department of Energy by Lawrence Livermore National Laboratory under Contract DE-AC52-07NA27344, and supported by the U.S. Department of Homeland Security under DNDO Contract HSHQDC-09-X-00554/0001. One of us (FVH) wishes to thank D.T. Santa Maria for important discussions on simulation optimization.

[1] G.A. Mourou, T.Tajima, S.V. Bulanov, Rev. Mod. Phys. 78, 309 (2006).

[2] T.O. Raubenheimer and F. Zimmermann, Rev. Mod. Phys. 72,

- 95 (2000).
- [3] A. H. Compton, Phys. Rev. 21, 483 (1921); G.R. Blumenthal and R.J. Gould, Rev. Mod. Phys. 42, 237 (1970).
- [4] D.J. Gibson, et al., Phys. Plasmas, 11, 2857 (2004).
- [5] F. Albert, et al., Opt. Letters, 35, vol. 3 354-357 (2010).
- [6] J. Arthur, G. Materlik, R. Tatchyn, and H. Winick, Rev. Sci. Instrum. 66,1987 (1995).
- [7] H. Von Garrel, et al., Phys. Rev. C, 73, 054315 (2006).
- [8] F.V. Hartemann, et al., Phys. Rev. E, 64, 016501 (2001).
- [9] G. Bhatt, et al., Phys. Rev. A, 28, 2195 (1983).
- [10] J.W. Meyer, Phys. Rev. D, 3, 621 (1971).
- [11] L.M. Brown and R. P. Feynman, Phys. Rev., 85, 231 (1952).
- [12] F.V. Hartemann, Phys. Rev. E, 61, 972 (2000)
- [13] F.V. Hartemann et al., Phys. Rev. E, 54, 2956 (1996)
- [14] <http://mathworld.wolfram.com/LaguerrePolynomial.html>
- [15] J.B. Rosenzweig, Fundamentals of beam physics, Oxford university press (2003).
- [16] F.V. Hartemann, et al., Phys. Rev. E, 58, 5001 (1998).